



UNIVERSITY
of
GREENWICH

Greenwich Academic Literature Archive (GALA)
– the University of Greenwich open access repository
<http://gala.gre.ac.uk>

Citation for published version:

Chen, Jinhu, Trevarthen, James A., Deng, Tong, Bradley, Michael S.A., Rahatekar, Sameer S. and Koziol, Krzysztof K.K. (2014) Aligned carbon nanotube reinforced high performance polymer composites with low erosive wear. *Composites Part A: Applied Science and Manufacturing*, 67. pp. 86-95. ISSN 1359-835X (doi:10.1016/j.compositesa.2014.08.009)

Publisher's version available at:

<http://dx.doi.org/10.1016/j.compositesa.2014.08.009>

Please note that where the full text version provided on GALA is not the final published version, the version made available will be the most up-to-date full-text (post-print) version as provided by the author(s). Where possible, or if citing, it is recommended that the publisher's (definitive) version be consulted to ensure any subsequent changes to the text are noted.

Citation for this version held on GALA:

Chen, Jinhu, Trevarthen, James A., Deng, Tong, Bradley, Michael S.A., Rahatekar, Sameer S. and Koziol, Krzysztof K.K. (2014) Aligned carbon nanotube reinforced high performance polymer composites with low erosive wear. London: Greenwich Academic Literature Archive.
Available at: <http://gala.gre.ac.uk/12030/>

Contact: gala@gre.ac.uk

Accepted Manuscript

Aligned carbon nanotube reinforced high performance polymer composites with low erosive wear

Jinhu Chen, James A. Trevarthen, Tong Deng, Michael S.A. Bradley, Sameer S. Rahatekar, Krzysztof K.K. Koziol

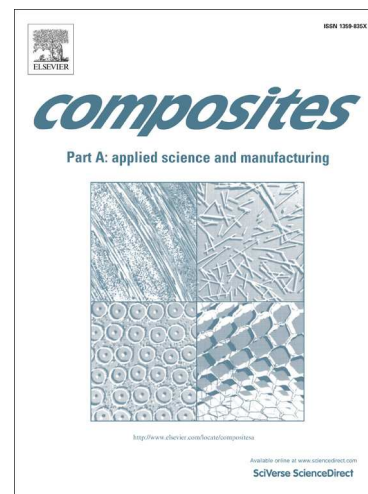
PII: S1359-835X(14)00242-5
DOI: <http://dx.doi.org/10.1016/j.compositesa.2014.08.009>
Reference: JCOMA 3685

To appear in: *Composites: Part A*

Received Date: 13 January 2014
Revised Date: 25 July 2014
Accepted Date: 9 August 2014

Please cite this article as: Chen, J., Trevarthen, J.A., Deng, T., Bradley, M.S.A., Rahatekar, S.S., Koziol, K.K.K., Aligned carbon nanotube reinforced high performance polymer composites with low erosive wear, *Composites: Part A* (2014), doi: <http://dx.doi.org/10.1016/j.compositesa.2014.08.009>

This is a PDF file of an unedited manuscript that has been accepted for publication. As a service to our customers we are providing this early version of the manuscript. The manuscript will undergo copyediting, typesetting, and review of the resulting proof before it is published in its final form. Please note that during the production process errors may be discovered which could affect the content, and all legal disclaimers that apply to the journal pertain.



Aligned carbon nanotube reinforced high performance polymer composites with low erosive wear

Jinhu Chen^a, James A. Trevarthen^b, Tong Deng^c, Michael S. A. Bradley^c, Sameer S. Rahatekar^b,
Krzysztof K. K. Koziol^{a,*1}

^a Department of Materials Science and Metallurgy, University of Cambridge, 27 Charles Babbage Road,
Cambridge CB3 0FS, UK

^b Advanced Composites Centre for Innovation and Science (ACCIS), Aerospace Engineering, University
of Bristol, Bristol BS8 1TR, UK

^c The Wolfson Centre for Bulk Solids Handling Technology, School of Engineering, University of
Greenwich, Chatham, ME4 4TB, UK

Abstract

The erosive wear behaviour of epoxy composites reinforced with aligned, as-produced carbon nanotube (CNT) films was investigated. The CNT film composites were fabricated in two different configurations, where the unidirectional (0°) and bi-directional (0°/90°) aligned CNT films were exposed to the particle stream. Results have shown that the unidirectional (0°) CNT film/epoxy composite exhibit superior erosive wear resistance compared to the unidirectional (0°) carbon fibre reinforced epoxy composite. Furthermore, the bi-directional (0°/90°) CNT film/epoxy composite shows even better resistance to erosion compared to the unidirectional (0°) CNT film/epoxy composite due to additional impact energy absorption resulted from CNT networks. Scanning Electron Microscopy (SEM) provides further insight into the erosive wear mechanisms of CNT film composites at different impingement angles. This work has successfully introduced aligned as-produced CNT films fabricating epoxy composites using

¹ Corresponding author: +44 1223 334356
E-mail addresses: kk292@cam.ac.uk (K. K. K. Koziol).

traditional composite manufacturing processes with low erosive wear and high electrical performance which deliver potential for engineering applications.

1. Introduction

Solid particle erosion is a dynamic process which involves the progressive loss of materials from a surface by means of impinging particles from various directions. This type of wear has been paid much attention as it causes severe problems including loss of efficiency, reduced performance and high maintenance costs in many industrial applications. For example, helicopter rotor blades and high-speed vehicles, whose surfaces are usually exposed to air which contains sharp and solid particles. Extreme conditions like sandy or dusty environments may even speed up the erosive wear process resulting in more damage.

Since the early 1980s, research studies on the solid particle erosive wear behaviour of materials have extended from metallic materials to fibre reinforced polymer composites [1], [2] and [3]. Fibre reinforced polymer composites provide extra benefits including lightweight, excellent specific stiffness and strength, freedom in design due to tailorable anisotropy [4], and these advantages contribute to various applications from daily-use appliances to high-tech engineering and aircraft systems. However, the erosive wear resistance has remained a major issue because polymer composites usually exhibit relatively poor resistance to erosion compared to metallic materials [3] and, in some cases, the presence of fibres reduces the erosion resistance of the polymer matrix [5] and [6]. Efforts have been made to design composite laminates reinforced with multi-directional fibres which help to absorb additional impact energy from solid particles, but the improvements in erosion resistance were found to be very limited in the case of both carbon fibres [7] and glass fibres [5].

Since the discovery of carbon nanotubes (CNTs) [8], their extraordinary multifunctional properties have stimulated great interest in polymer composites reinforced with CNTs. Particularly, due to their graphitic structure, CNTs exhibit lubricating behaviour [9], [10], [11] and [12] which is reported to make significant improvements to the abrasive wear resistance of CNT based nanocomposites [13] and [14]. However, the erosive wear resistance of CNT based polymer composites has received much less attention due to the developing stage of CNT synthesis as well as the manufacturing difficulties in production of

bulk polymer composites containing a high loading fraction of CNTs. The erosive wear performance of epoxy composites reinforced with aligned CNT arrays synthesized by substrate-grown CVD method has only recently been reported [15]. In this paper, the presence of vertically aligned CNT arrays within epoxy matrix gives improved erosion resistance which opens up a new way for erosive wear applications of polymer composites using aligned CNTs. Inspired by this work, CNTs films synthesized by the continuous CVD process [16] can be assembled together to fabricate uni- or multi-directional CNT film/epoxy based composites. Such CNT structures can then be mechanically comparable to conventional fibre reinforced polymer composites. To date, the incorporation of multi-layered CNT films in an epoxy matrix has produced composites with significantly improved fracture toughness and Young's modulus [17].

In the present work we investigate the erosive wear behaviour of epoxy based composites reinforced with as-produced, uncondensed CNT films. The CNT film epoxy composites were prepared in two different nanotube alignment configurations, where CNT films within the epoxy matrix were stacked either unidirectionally (0°) or bidirectionally ($0^\circ/90^\circ$) in order to investigate the effect of CNT film orientations on the erosive wear behaviour of epoxy based composites. In addition, unidirectional (0°) carbon fibre/epoxy composites were also fabricated for comparison.

CNTs used in this work were synthesised using the direct-spinning CVD method, from which continuously long CNTs were collected onto the rotational drawer, forming CNT films. A vacuum bagging system was set up to fabricate both unidirectional (0°) and bi-directional ($0^\circ/90^\circ$) CNT film/epoxy composites.

This work demonstrates methods to investigate the erosive wear resistance of epoxy composites reinforced with a high loading fraction of aligned CNT films. Results have shown that the two types of CNT film reinforced epoxy composites exhibit superior erosive wear resistance compared to unidirectional (0°) carbon fibre reinforced epoxy composites. In particular, the bidirectional CNT films within the epoxy matrix will absorb additional impact energy from solid particles, resulting in improved erosion resistance. The erosive wear mechanisms of composites were further investigated at various impingement angles using SEM analysis. In addition, the aligned CNT film reinforced epoxy composites

with high electrical conductivity also provide an exciting opportunity for multifunctional purposes such as lightweight lightning strike protection [18].

2. Materials and methods

2.1. CNT synthesis and characterisation

Carbon nanotubes used in the study were synthesised *via* continuous CVD process [16]. Methane was used as the hydrocarbon feedstock and was injected into the hot furnace (1300°C) along with ferrocene and thiophene. CNTs start to grow in the furnace and form an aerogel, which can be mechanically drawn out of the furnace. In this way, CNT films were produced by continuously collecting CNTs onto the rotational winder until the winder was fully covered. Typical collection time is about 1 hour. The average thickness of the CNT films collected from the winder after 1 hour of spinning was 30-50 µm. CNTs synthesised in this study are mainly multi-walled nanotubes. The quality of CNT films (I_D/I_G ratio) was characterized by Raman spectroscopy using a Renishaw Ramanscope 1000 system with $\lambda=633$ nm laser (Fig. S1). The alignment of CNT films was observed using SEM analysis (JEOL 6340F) (Fig. S2). Transmission Electron Microscopy (TEM) images of CNT films are shown in Fig. S3.

2.2. Composite preparation and characterisation

CNT films were originally collected onto a sheet of A4 paper. To begin with, the CNT films were cut into long, rectangular strips 25mm in width to be ready for the film stacking, with nanotubes aligned along the long axis. Unidirectional stacks of CNT film were produced by folding these long strips at 25mm intervals along the long axis, with the aid of tweezers. Bidirectional stacks were formed by cutting long CNT strips at 25mm intervals and stacking them in alternate orientations of 0° and 90° (Fig. 1).

A two-component, hot-curing epoxy system was used in this work: Araldite LY 556 and Hardener XB 3473 (supplied by Mouldlife Ltd). Araldite LY 556 is a bisphenol-A based standard epoxy resin with typical viscosity of 10000-12000 mPa·s at 25 °C. XB 3473 is a formulated amine-based hardener.

The epoxy resin and its hardener were thoroughly mixed in a weight ratio of 100:23 by weight, using a high shear mechanical mixer (Silverson L4R). A degassing procedure was then carried out on the mixed

resin using a vacuum oven to remove entrapped air bubbles. The mixed epoxy/hardener was pre-heated to 60 °C during degassing and infiltration to decrease the viscosity of the mixture in order to assist gas escape and CNT film wetting.

To combine epoxy resin and CNT, CNT film stacks were placed in a silicone rubber mould with 25mm x 25mm cavity, into which the degassed, pre-heated epoxy resin/hardener was slowly cast. Once films were fully immersed, the mould was placed into an oven at 60 °C for 1 hour to ensure sufficient infiltration.

A vacuum bagging system (Fig. 2) was applied to make both carbon fibre and uni/bi-directional CNT-film/epoxy composites. To produce this, an ETFE release film, perforated at P3 intervals (pin pricked every 8mm) with 15µm thickness (supplied by Vac Innovation Ltd), was cut into the same square format (25mm x 25mm) as the stacked CNT films, and placed over the infiltrated CNT-films. The silicone rubber mould containing infiltrated CNT-films along with perforated release films was placed into a pink nylon vacuum bagging tube, 305mm in width (VACTiteUltraP12 supplied by Vac Innovation Ltd.). This was covered by two layers of breather fabric (lightweight polyester 150g/m² with 2.5mm thickness). This enables any excessive resin to be squeezed out from the composite via the perforated release films, through the holes, and absorbed by the breather fabrics during the vacuum bagging process, improving the loading fractions of CNTs.

Exactly the same vacuum bagging set-up was used when fabricating unidirectional (0°) carbon fibre reinforced epoxy composites.

Finally, the vacuum bagging tube was sealed using a sealant tape, and connected to a vacuum pump (Edwards 8 E2M8 vacuum pump, 1×10⁻³ mbar). Standard curing procedure (2 hours at 120°C + 2 hours at 140°C + 2 hours at 180°C) was followed and the vacuum applied throughout the curing process.

For comparison, carbon fibre T-300 (supplied by Toray Industries Inc.) with typical tensile strength of 3530 MPa and tensile modulus of 230 GPa was also used to fabricate unidirectional (0°) epoxy composites using the composite fabrication procedure described above. All polymer and polymer composite samples were further polished to achieve the same surface finish of with asperities of ≤6µm in size.

The weight fractions of carbon fibres and CNT films within epoxy composites were measured using Thermogravimetric Analysis (TA Instruments Q500), with typical sample weights of 5mg and heating rate of 10 °C/min under nitrogen atmosphere (Fig. S4).

2.3. Erosion testing methodology

A centrifugal acceleration type erosion tester was used to carry out the erosion tests in this work whose schematic diagram is shown in Fig. S5. This type of erosion tester relies upon the solid particles travelling through radially positioned tubes within the rotating disc accelerated by the centrifugal force. The samples were attached onto a target holding system around the rotating disc which can be adjusted at various impingement angles. The test parameters are summarized in **Error! Reference source not found.**

In this work, a specific erosion rate is defined as mass removed from the surface of a material divided by total mass of eroding particles impinging on the surface. The erosion rate was calculated by using a computational model [18] based on particle dynamics within the tester such as particle shape and size, particle concentration in the fluid stream and particle velocities [20] and [21].

Olivine sands were used as eroding particles in this study. They are angular shaped with median grain size (D50) of 238µm measured by granulometric analysis (Fig. 3a-b). Particle impact velocity was 40 m/s throughout the erosion tests. Four impingement angles were studied to explore erosive wear behaviour of the composites: 20°, 30°, 45° and 90°. From Fig. 4a, the horizontal component of the particle flow axis was parallel to the alignment direction of stacked unidirectional (0°) carbon fibre/CNT films within the epoxy composites. From Fig. 4b, the horizontal component of the particle flow axis was perpendicular to one of the alignment direction of bidirectional CNT films. Repeatability was ensured by testing two samples of the same kind of material within a single run of erosion test. At least 6 runs of erosion tests were carried out to ensure the target materials reached their steady state erosion rates. The eroded materials were cleaned using ethanol under sonication for 15 minutes to remove any embedded sand particles, and further dried in an oven at 80°C. Then the mass of the target materials was weighed to an accuracy of 0.1 mg using an analytical balance. The mass loss values of the eroded materials for the

whole set of erosion tests were measured in the same sequence to eliminate experimental errors such as moisture absorption.

After erosion testing, the eroded surfaces of the epoxy composites were examined by using Scanning Electron Microscopy (JEOL-6340F and JEOL-5800F) to investigate the erosive wear mechanism at different impingement angles. To help distinguish the difference between un-eroded and eroded surface, the erosion scar of the chosen target materials (neat epoxy and unidirectional (0°) CNT film/epoxy composites) at the impingement angles of 20°, 30° and 90° is shown in Fig. S6.

2.4. Electrical characterisation

The electrical conductivity measurements were carried out on all the epoxy composite samples using a 2-point probe setup (Keithley 2000 multimeter). The composite samples were cut into rectangular-shaped strips (5 mm x 15 mm) and polished to achieve uniform thickness of 1.5 mm. A conductive silver paste was used to coat the opposite sides of the composite sample to ensure good contact during measurements. The electrical conductivity σ was calculated using the equation:

$$\sigma = L/(R \times A)$$

, where R is the resistance measured over length L , and A is the cross-sectional area of the sample coated with silver paste.

3. Results and discussion

3.1. Erosion performance

A series of erosion tests were carried out to assess the effect of two alignment configurations of CNT films in the epoxy matrix on the erosive wear behaviours. The results were compared to unidirectional (0°) carbon fibre epoxy composite and neat epoxy (Fig. 5a-b).

Fig. 5a shows the erosion rates as a function of impingement angles. Ductile and brittle erosion behaviour can be clearly differentiated from this diagram. The maximum erosion rate of unidirectional (0°) carbon fibre/epoxy composite appears at an impingement angle of 90°, which reflects typical brittle erosion behaviour, whereas the two types of CNT-film/epoxy composites along with the neat epoxy exhibit maximum erosion rates in the range of 30° to 45°, showing ductile erosion behaviour. The incorporation

of carbon fibres reduces the erosion resistance of its epoxy matrix to a considerable extent, and changes the erosive wear behaviour of the neat epoxy due to the brittle nature of carbon fibres. For comparison, the erosion rates of unidirectional (0°) carbon fibre/epoxy composites were increased by 40%, 83%, 160% and 400% from 20° to 90° , respectively. On the other hand, unidirectional (0°) CNT-film/epoxy composite shows slightly worse resistance to erosion compared to neat epoxy except at 20° impingement angle (Fig. 5b), and neat epoxy exhibits better erosion resistance at the rest of the three impingement angles. Moreover, bidirectional ($0^\circ/90^\circ$) CNT film/epoxy composites exhibit better erosion resistance than that of neat epoxy: the erosive wear resistance was improved by 18% at 20° impingement angle and 6% at 90° impingement angle, whereas there were no improvements at the impingement angles of 30° and 45° . Compared to unidirectional (0°) CNT film/epoxy composites, the erosive wear resistance of bidirectional composites was improved by 13%, 10%, 5% and 15% at the impingement angles from 20° to 90° , respectively. It can be estimated that CNT films with bidirectional structure may absorb more impact energy from impinging eroding particles, which leads to improved erosive wear resistance. In addition, the results show a dependence on the alignment geometries of CNT films within the epoxy matrix: bidirectional CNT films show better resistance to erosion compared to the unidirectional CNT films. Further explanation can be found in SEM analysis.

3.2. SEM analysis on eroded surface of unidirectional (0°) carbon fibre/epoxy composite

The eroded surface of unidirectional (0°) carbon fibre/epoxy composite was observed by SEM analysis in order to investigate the mechanism on the brittle erosion behaviour at different impingement angles. The surface morphology of the uneroded composite sample shows very good alignment directions of intact carbon fibres embedded within the epoxy matrix (Fig. 6).

Fig. 7a-d shows the eroded surfaces of carbon fibre/epoxy composite samples at 20° , 45° and 90° . The typical brittle erosion behaviour where maximum erosion rate occurs at 90° can be reflected from the surface morphology. At 20° where impinging sand particles had small perpendicular components of velocity to the surface, the epoxy matrix was chipped away by the abrasive action of particles revealing carbon fibres. Fewer fibres were broken and eroded away by cutting action, but most of the fibres were kept almost firmly in place and good adhesion seen between epoxy matrix and fibres. At 45° , where a high erosion rate was found, the sand particles resulted in increased numbers of broken fibres revealing

long cavities as well as small flakes. At 90° , direct impact from sand particles resulted in the highest kinetic energy which was dissipated by a large amount of micro-cracking and plastic deformation of carbon fibres. Interfacial debonding between fibres and matrix was also observed. Due to multiple impacts, the brittle nature of carbon fibres formed small wear debris but still attached to the surface. Particularly from Fig. 7d under zoom-out view, a long and deep crater was formed at 90° which indicated that intense breakage and debonding of carbon fibres due to direct impacts was not sufficiently supported by the epoxy matrix causing larger removal of material.

3.3. SEM (low-magnification) analysis on eroded unidirectional (0°) CNT film/epoxy composites

In order to understand the interaction between erodent particles and the composite surface at different impingement angles, the surface morphology of the eroded CNT film/epoxy composites was observed using SEM at micron-scale. As discussed above, both unidirectional (0°) and bidirectional ($0^\circ/90^\circ$) CNT film/epoxy composites behaved ductile erosion where the maximum erosion rates occurred in the range 30° to 45° . Therefore, similar surface morphology was investigated by SEM under lower magnification.

Fig. 8a-d shows the eroded surface of unidirectional (0°) CNT film/epoxy composite under low magnification. Thin layers of materials were chipped off from the surface at 20° impingement angle due to significant cutting effects (Fig. 8a). At this angle, the cutting action of sand particles formed a lot of 'lips' which were shown as white features. Those lips tend to align towards the impingement direction of sand particles. With the increasing impingement angle, more plastic deformation resulted in high erosion rates because of brittleness of the materials. At high impingement angles, because larger pieces of surface materials were chipped off, the lip formations could no longer be observed which made it more difficult to distinguish lip formations under certain directions where part of the surface areas were plastically deformed and flattened forming platelets (Fig. 8c). The platelets became thinner and more vulnerable to erosion from continual impacts of sand particles. At an impingement angle of 90° , instead of the lips or platelets observed at 20° and 45° , direct impact of sand particles caused larger plastic deformation of the matrix materials forming deep cavities instead of the removal and breakage of the materials as brittle behaviour, and this reflects typical ductile erosion behaviour obtained from the previous erosion rate comparisons. Compared to that of unidirectional (0°) carbon fibre epoxy composites at 90° , very little wear debris can be seen adhering to the surface (Fig. 8d). It is not possible to observe any nanotubes on

the material surface at such low magnification. Therefore, to understand the erosive wear mechanism of the two types of CNT-film reinforced epoxy composites, it is essential to explore how CNTs interacted with impinging sand particles as well as the dependence on the alignment geometries of CNTs at four impingement angles, using high magnification SEM analysis.

3.4. SEM (high-magnification) analysis on eroded unidirectional (0°) CNT-film/epoxy composites

High magnification SEM analysis provides further insight into the surface morphology of the eroded surface as well as the erosive wear mechanism of CNTs.

Fig. 9a shows a wear scar at the end of the 'lip' structure, which is the area where the surface materials were chipped off by sand particles. The CNTs maintained good bonding with the epoxy matrix without any nanotube extrusion and debonding of the epoxy matrix. Fig. 9b shows a closer view of the 'lip' structure described previously at 20° impingement angle. Series of roughly parallel slip bands are visible on the right-hand side, and the sand particles generated a new crater by means of plastic deformation. Then slip bands occurred due to the subsequent impacts on the wall of the existing craters forming a new crater adjacent to the old one. Those slip bands extended deeper until a final crater was formed. A similar type of erosion mechanism was also reported on the surface of ductile metals [22]. Clearly both the length of the slip band and the general CNT alignments follow the impact direction of the sand particles. Also there is no bridging of CNTs connecting the sides of slip bands.

Fig. 9c-d shows the eroded surface morphology at 45° impingement angle. Deeper crater was found as a result of plastic deformation by particle impacts. The high impact energy caused many small pieces of matrix materials to be chipped off (Fig. 9c) which led to high erosion rates. From Fig. 9d, some wear debris can be observed adhered on the surface which appears to consist only of epoxy matrix without any embedded CNTs. The intense chipping action of eroding particles made CNTs debonded from matrix materials forming craters along with remaining debris.

At impingement angle of 90° , except the deep craters, multiple impacts of sand particles also caused micro to macro-cracking, and produced separate blocks of matrix materials (Fig. 9e). CNT filaments were pulled out between these blocks, but remained connected at each performing a 'bridging' function (Fig. 9e). This function certainly helps to protect the 'blocks' from being eroded away. Fig. 9f shows a triangle

shaped crater which indicates that a piece of surface material is chipped off entirely. Thus, the CNTs underneath were revealed (Fig. 9f). In this case, the epoxy matrix can be eroded away more easily than embedded CNTs resulting in the debonding between CNTs and matrix. It is believed that CNTs absorb additional energy that reduces the erosion of matrix materials. On the other hand, a lateral crack is formed from the side of the crater which is a characteristic for erosion under high impingement angles (Fig. 9f).

3.5. SEM (high-magnification) analysis on eroded bi-directional (0°/90°) CNT film/epoxy composites

Different erosive wear mechanism was observed for bidirectional (0°/90°) CNT film/epoxy composites by using high magnification SEM analysis, which correlates with improved erosion resistance on this type of CNT film composite discussed previously.

At 20°, entangled CNT networks were found between the sidewall and the surface of the crater, which showed a different erosive wear mechanism compared to that of the unidirectional (0°) CNT-film/epoxy composite (Fig. 10a). Sand particles stroke on the surface/crater where CNTs within the matrix aligned parallel to the impinging direction, and this deformed the epoxy matrix as well as revealing the next ply of CNTs, aligned vertically to the exposed surface. The exposed CNTs were further stretched by tensile force connecting to the new crater zone after subsequent impacts. As mentioned previously, this bidirectional 'bridging' function helps to improve resistance to erosion. Fig. 10b shows clear evidence that the separation of the matrix material upon impact was resisted by the bridging of multiple nanotube filaments.

At 45°, separated blocks or pieces of surface materials without CNT bridging were observed due to the intense chipping action of eroding particles (Fig. 10c). In another case, the presence of CNT films offered extra flexibility of the material which provided a cushion effect upon subsequent impact (Fig. 10c). Fig. 10d shows the edge of a platelet which was eroded by means of the breakage of CNT networks. Therefore at this angle, the embedded CNT networks may still not tolerate the high energy impact, thus leading to the nanotube fracture.

From Fig. 10e, a number of wear debris are found at 90° impingement angle. These wear debris contain both matrix materials and CNTs connected to each other by means of extruded CNT filaments. Fig. 10f shows further evidence of the plastic deformation of matrix materials containing cross-ply CNT

networks around the edge of a crater. Therefore, it can be concluded that the bidirectional CNT networks within the epoxy matrix will increase the probability of nanotube bridging, which will absorb more impact energy of sand particles and reduce the erosive damage of the surface.

3.6. Electrical conductivity of epoxy composites

As seen in Fig. 11, the electrical properties of unidirectional carbon fibre and CNT film based epoxy composites were found to be highly anisotropic. Moreover, the highest conductivity value (2767.46 ± 147.42 S/m) was measured on unidirectional CNT film/epoxy composite (along CNT alignment) which was over 3 times higher than that of unidirectional carbon fibre/epoxy composite (along fibre direction). All values are presented in Tab. S1. It is also important to note that lower weight fractions of aligned CNT films within the epoxy matrix, whether bidirectional configuration (14 wt.%) or perpendicular to the unidirectional CNT film alignment (15 wt.%), will result in similar electrical performance level compared to that of epoxy composites containing 68 wt.% of carbon fibres along the fibre direction. To summarize, the good electrical performance of CNT film based epoxy composites is an additional benefit for using these materials, which provides very high potential in the applications of electrostatic dissipation and lightning strike protection.

4. Conclusions

The effect of CNT film reinforced structures on erosive wear performance of epoxy composites has been investigated. The aligned, as-produced CNT films were stacked in two alignment configurations: unidirectional (0°) and bidirectional ($0^\circ/90^\circ$). The experimental results show that the two types of CNT film reinforced epoxy composites have the same ductile erosive wear behaviour as neat epoxy where their erosion rates peak at the impingement angle of 30° - 45° . Their erosion resistance is superior to that of the unidirectional (0°) carbon fibre/epoxy composite prepared under identical manufacturing techniques. The unidirectional (0°) carbon fibre/epoxy composite has brittle erosive wear behaviour and here the erosion rate peaks at the impingement angle of 90° . SEM analysis shows that CNTs maintain good interfacial adhesion with epoxy matrix at shallow impingement angle for the unidirectional (0°) CNT film reinforcement. At high impingement angle, micro-cracks were formed and transferred into multiple blocks of matrix materials which were partially connected by nanotubes. Bidirectional ($0^\circ/90^\circ$) CNT

film/epoxy composite shows slightly better erosion resistance which can be attributed to the ability of CNT networks to absorb additional impact energy of erodent particles. As a result, the presence of CNT film delivers the resistance to erosion by means of CNT bridging and stretching. Also at high impingement angle, SEM analysis shows that the bonding between CNT films and epoxy matrix is relatively weak after multiple impacts.

It is worth noting that when replacing carbon fibres with aligned CNT films as the reinforcement material, the embedded CNTs demonstrate the ability to change erosive wear behaviour from brittle to ductile. Due to the good toughness and ductility, CNTs can absorb more energy upon fracture or bending. It may be possible to further increase the erosive wear resistance of these composites by applying mild functionalisation of CNTs, which is expected to improve interaction between aligned CNTs and epoxy matrix.

This work demonstrates great potential for the aligned CNTs as future reinforcement materials either replacing carbon fibres in the polymer matrix or as an addition to the carbon fibres composites, by addition of a thin carbon nanotube composite coating onto the traditional carbon fibre composite. This would offer superior erosive wear protection and significant improvement in electrical performance.

Acknowledgements

K. K. K. Koziol and J. Chen thank the Royal Society for financial support of this work. J.A. Trevarthen gratefully acknowledges the support of the EPSRC under its ACCIS Doctoral Training Centre, grant EP/G036772/1.

References

- [1] Zahavi J. Solid particle erosion of reinforced composite materials. *Wear* 1981; 71(2): 179-90.
- [2] Zahavi J. Schmitt GF. Solid particle erosion of polymeric coatings. *Wear* 1981; 71(2): 191-210.
- [3] Pool KV, Dharan CKH, Finnie I. Erosive wear of composite materials. *Wear* 1986; 107(1): 1-12.
- [4] Hull D, Clyne TW. An introduction to composite materials. 2nd ed. Cambridge University Press, 1996.
- [5] Harsha AP, Jha SK. Erosive wear studies of epoxy-based composites at normal incidence. *Wear* 2008; 265(7-8):1129-35.

- [6] Tsuda K, Kubouchi M, Sakai T, Saputra AH, Mitomo N. General method for predicting the sand erosion rate of GFRP. *Wear* 2006; 260(9-10):1045-52.
- [7] Kim A, Kim I. Solid particle erosion of CFRP composite with different laminate orientations. *Wear* 2009; 267(11):1922-26.
- [8] Iijima S. Helical microtubules of graphitic carbon. *Nature* 1991; 354:56-8.
- [9] Kolmogorov AN, Crespi VH. Smoothest bearings: interlayer sliding in multiwalled carbon nanotubes. *Phys Rev Lett* 2000; 85:4727-30.
- [10] Cumings J, Zettl A. Low-friction nanoscale linear bearing realized from multiwall carbon nanotubes. *Science* 2000; 289:602-4.
- [11] Kis A, Jensen K, Aloni S, Mickelson W, Zettl A. Interlayer forces and ultralow sliding friction in multiwalled carbon nanotubes. *Phys Rev Lett* 2006; 97:025501.
- [12] Hirata A, Yoshioka N. Sliding friction properties of carbon nanotube coating deposited by microwave plasma chemical vapour deposition. *Tribol Int* 2004; 37(2004):893-8.
- [13] Jacobs O, Xu W, Schädel B, Wu W. Wear behaviour of carbon nanotube reinforced epoxy resin composites. *Tribol Lett* 2006; 23:65-75.
- [14] Cai H, Yan F, Xue Q. Investigation of tribological properties of polyimide/carbon nanotube nanocomposites. *Mat Sci Eng: A* 2004; 364(1-2):94-100.
- [15] Chen J, Hutchings IM, Deng T, Bradley MSA and Koziol KKK. The effect of carbon nanotube orientation on erosive wear resistance of CNT-epoxy based composites. *Carbon* 2014; 73:421-31.
- [16] Koziol K, Vilatela J, Moiala A, Motta M, Cunniff P, Sennett M, Windle A. High-performance carbon nanotube fiber. *Science* 2007; 318: 1892-1895.
- [17] Cheng Q, Li M, Jiang L, Tang Z. Bioinspired layered composites based on flattened double-walled carbon nanotubes. *Adv Mat* 2012; 24(14):1838-43.
- [18] Gagné M, Therriault D. Lightning strike protection of composites. *Prog Aerosp Sci* 2013, in press.
- [19] Deng T, Bradley MSA, Bingley MS. An investigation of particle dynamics within a centrifugal accelerator type erosion tester. *Wear* 2001; 247(1):55-65.
- [20] Li J, Deng T, Bingley MS, Bradley MSA. Prediction of particle rotation in a centrifugal accelerator erosion tester and the effect on erosion rate. *Wear* 2004; 258(1-4):497-502.

- [21] Deng T, Bingley MS, Bradley MSA. Influence of particle dynamics on erosion test conditions within the centrifugal accelerator type erosion tester. *Wear* 2001; 249(12):1059-69.
- [22] Bellman R, Levy A. Erosion mechanism in ductile metals. *Wear* 1981; 70(1):1-27.

ACCEPTED MANUSCRIPT

Fig. 1. Schematic images showing the procedure of stacking bidirectional CNT films (left) and unidirectional CNT films (right).a.

Fig. 2. A vacuum bagging system set-up for the fabrications of CNT film/epoxy and carbon fibre/epoxy composites.

Fig. 3. (a) SEM image of angular shaped olivine sands used for erosion testing; (b) The cumulative percentage of total mass of olivine sands [15].

Fig. 4. Schematic diagram of impingement angle and particle flow axis during erosion tests: (a) Unidirectional (0°) CNT film/carbon fibre reinforced epoxy composite; (b) bidirectional ($0^\circ/90^\circ$) CNT film/epoxy composite.

Fig. 5. (a) Steady state erosion rates of unidirectional (0°) carbon fibre/epoxy composite, unidirectional (0°) CNT film/epoxy composite, bidirectional ($0^\circ/90^\circ$) CNT film/epoxy composite and neat epoxy samples at impingement angles of 20° , 30° , 45° and 90° ; (b) Zoom-in to the part of the steady state erosion rates of CNT film/epoxy composites and neat epoxy.

Fig. 6. SEM micrographs of the polished surface of unidirectional (0°) carbon fibre/epoxy composite prior to erosion tests.

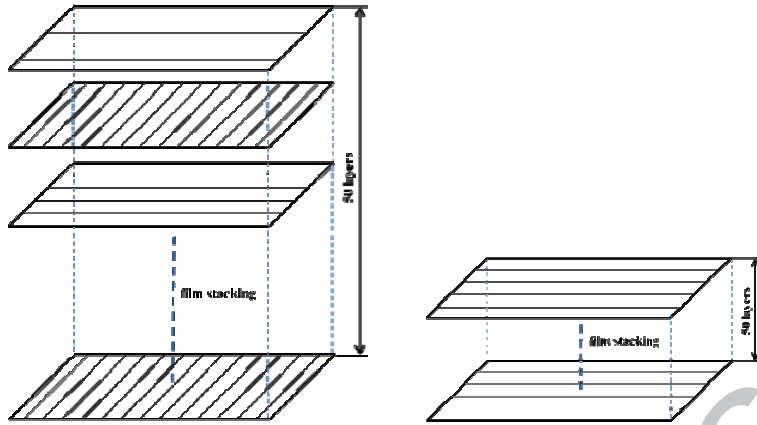
Fig. 7. SEM micrographs of eroded unidirectional (0°) carbon fibre/epoxy composite at impingement angles of (a) 20° (b) 45° (c) 90° (d) 90° (zoom out). Yellow arrow indicates the impingement direction with respect to the sample surface.

Fig. 8. SEM micrographs of eroded unidirectional (0°) CNT film/epoxy composites at impingement angles of (a) 20° (b) 45° (c) 90° (d) 90° (zoom in).

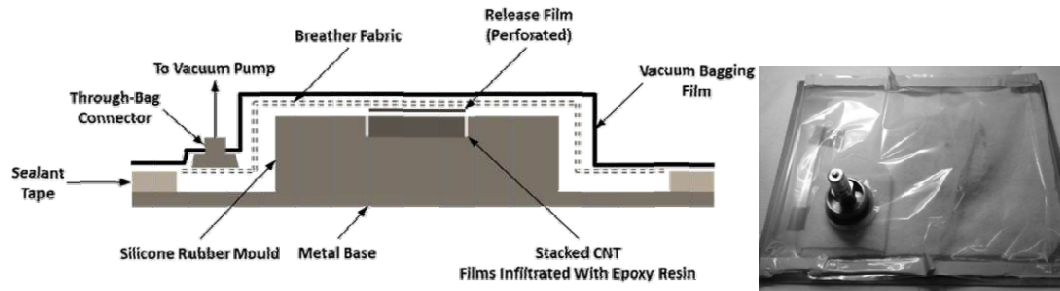
Fig. 9. High magnification SEM micrographs of eroded unidirectional (0°) CNT film/epoxy composites at impingement angles of (a)(b): 20° ; (c)(d): 45° ; and (e)(f): 90° .

Fig. 10. High magnification SEM micrographs of eroded bidirectional ($0^\circ/90^\circ$) CNT film/epoxy composites at impingement angles of (a)(b): 20° ; (c)(d): 45° ; and (e)(f): 90° .

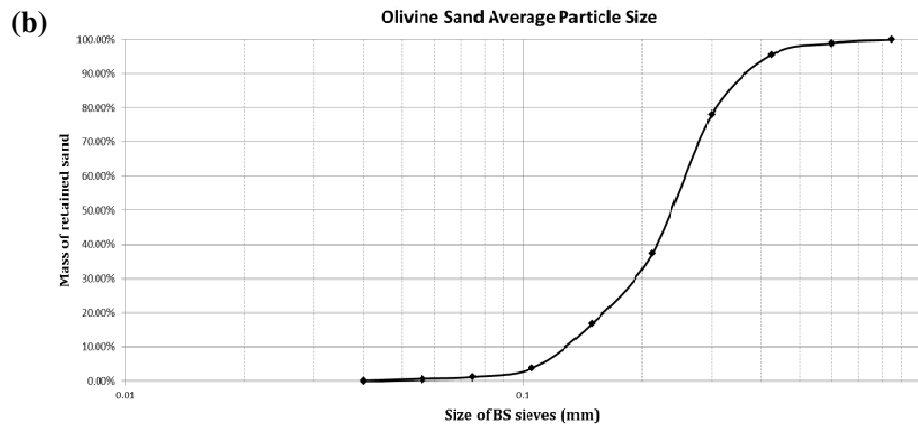
Fig. 11. Electrical conductivities of CNT film/epoxy composites and carbon fibre/epoxy composites.



ACCEPTED MANUSCRIPT

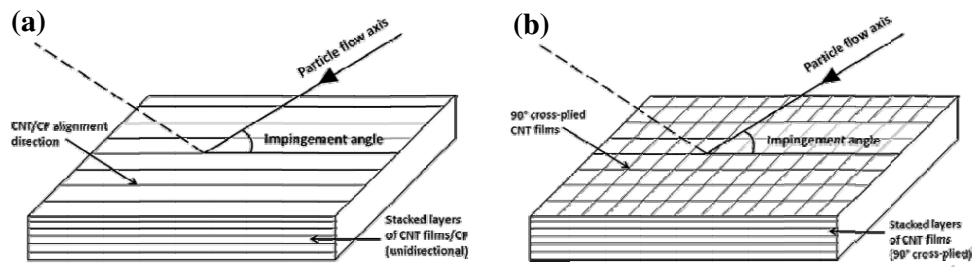


ACCEPTED MANUSCRIPT

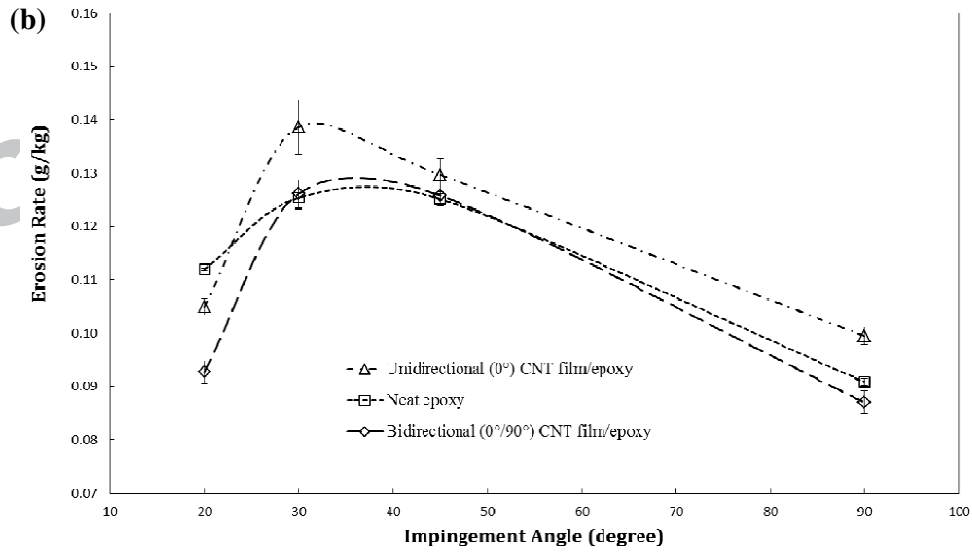
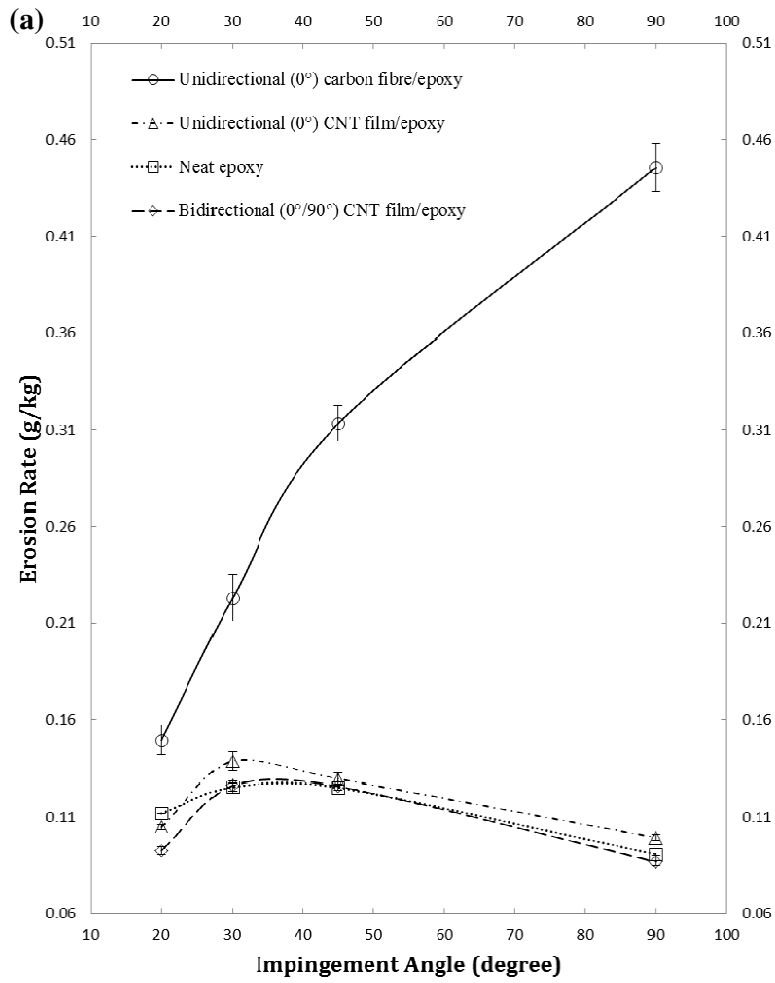


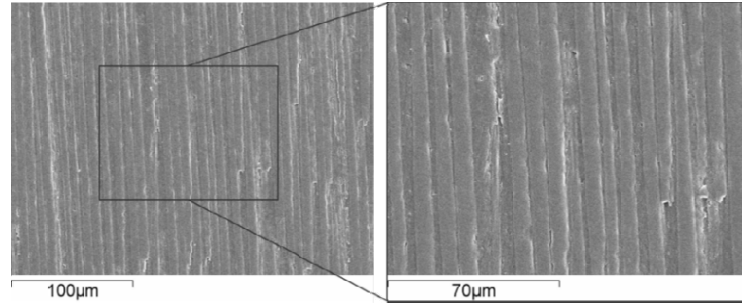
ACCEPTED

SCRIPT

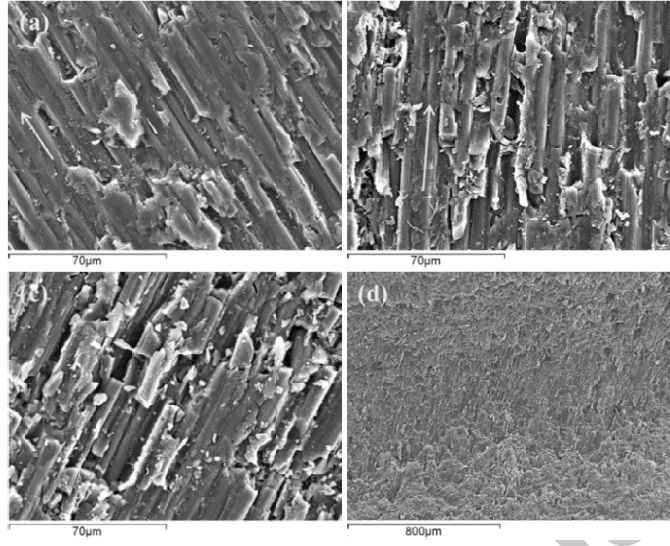


ACCEPTED MANUSCRIPT

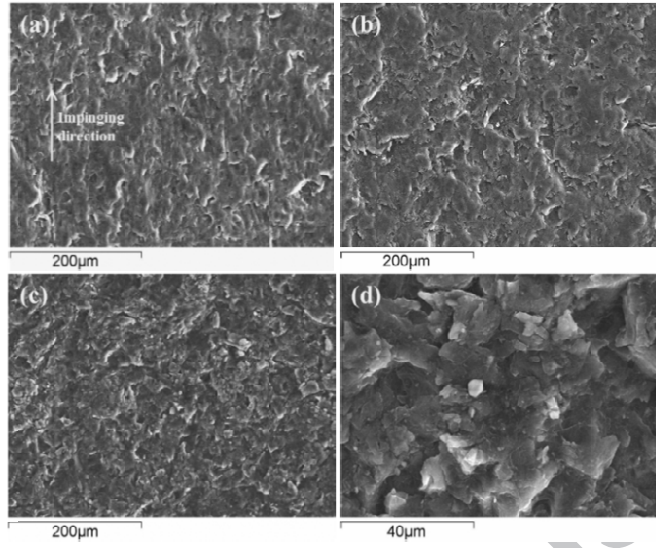




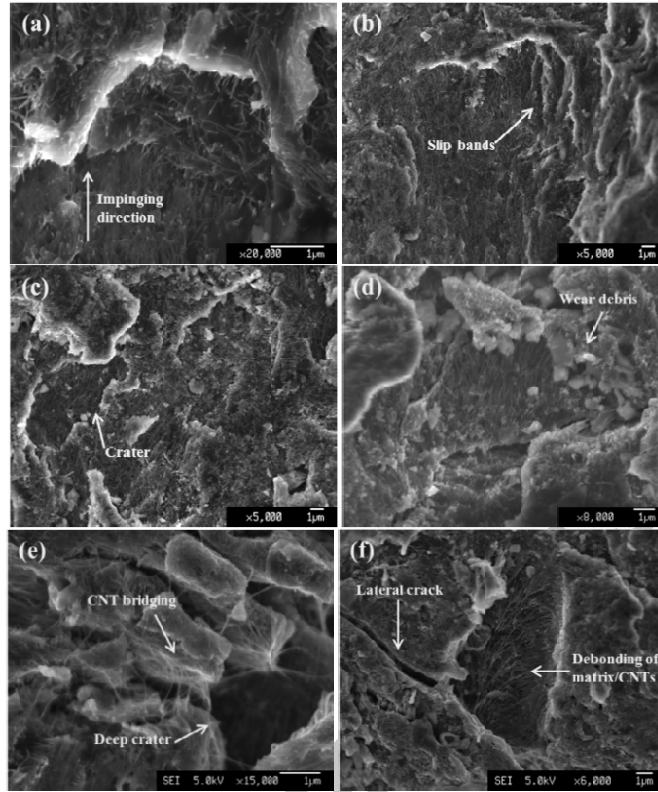
ACCEPTED MANUSCRIPT

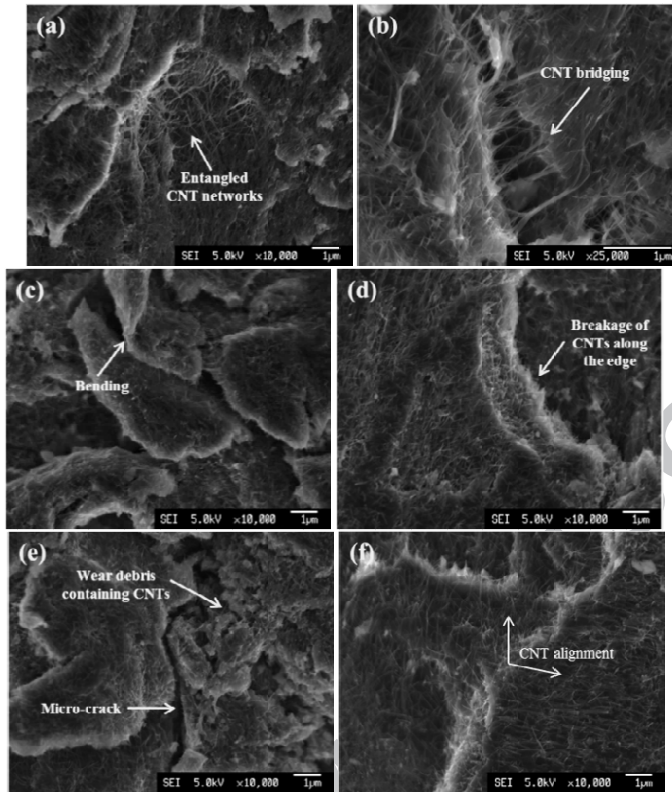


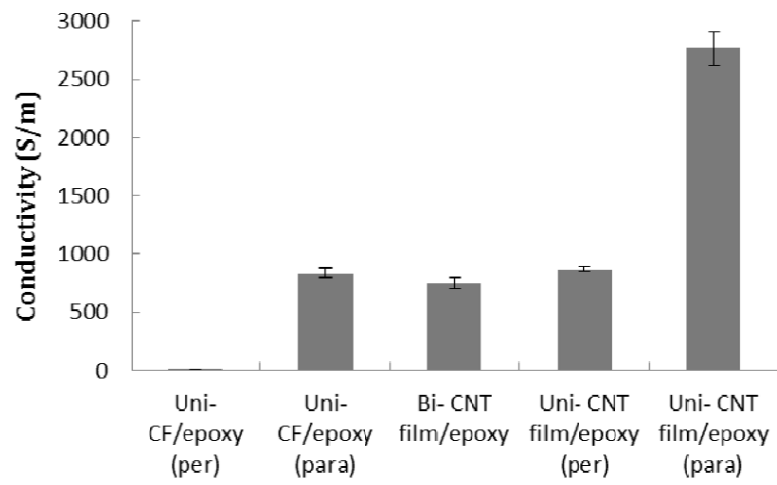
ACCEPTED MANUSCRIPT



ACCEPTED MANUSCRIPT







ACCEPTED MANUSCRIPT

Table 1. Erosion test conditions.

Test parameters	
Erodent	Olivine sands
Erodent size distribution D50 (μm)	238
Erodent shape	Angular
Erodent density (g/m^3)	3.28
Hardness of erodent (Mohs scale)	6.5-7.0
Impingement angles	20°, 30°, 45°, 90°
Impact velocity (m/s)	40
Particle flow feeding rate (kg/min)	0.125
Test temperature	Room temperature (20 °C)